



# Color optimization of single emissive white OLEDs via energy transfer between RGB fluorescent dopants



Nam Ho Kim<sup>a</sup>, You-Hyun Kim<sup>a</sup>, Ju-An Yoon<sup>a</sup>, Sang Youn Lee<sup>a</sup>, Dae Hyun Ryu<sup>b</sup>, Richard Wood<sup>c</sup>, C.-B. Moon<sup>a</sup>, Woo Young Kim<sup>a,c,\*</sup>

<sup>a</sup> Department of Green Energy & Semiconductor Engineering, Hoseo University, Asan, South Korea

<sup>b</sup> Department of Information Technology, Hansei University, Gunpo, South Korea

<sup>c</sup> Department of Engineering Physics, McMaster University, Hamilton, Ontario, Canada L8S 4L7

## ARTICLE INFO

### Article history:

Received 12 March 2013

Received in revised form

24 May 2013

Accepted 30 May 2013

Available online 20 June 2013

### Keywords:

White OLED

Single emissive

Color coordinates

Energy transfer

Fluorescent dopant

## ABSTRACT

The electroluminescent characteristics of white organic light-emitting diodes (WOLEDs) were investigated including single emitting layer (SEL) with an ADN host and dopants; BCzVBi, C545T, and DCJTb for blue, green and red emission, respectively. The structure of the high efficiency WOLED device was; ITO/NPB(700 Å)/ADN: BCzVBi-7%:C545T-0.05%:DCJTb-0.1%(300 Å)/Bphen(300 Å)/LiQ(20 Å)/Al(1200 Å) for mixing three primary colors. Luminous efficiency was 9.08 cd/A at 3.5 V and Commission Internationale de L'éclairage (CIE<sub>x,y</sub>) coordinates of white emission was measured as (0.320, 0.338) at 8 V while simulated CIE<sub>x,y</sub> coordinates were (0.336, 0.324) via estimation from each dopant's PL spectrum.

© 2013 The Authors. Published by Elsevier B.V. Open access under [CC BY-NC-ND license](http://creativecommons.org/licenses/by-nc-nd/3.0/).

## 1. Introduction

The multilayer organic light emitting diode was first demonstrated by Tang and Vanslyke in 1987 [1]. Organic light-emitting diodes (OLEDs) attract a high level of research enthusiasm due to their thin-film aspects, high-contrast, light-weight, fast-response, wide-view-angle and low-voltage attributes. They have been regarded as one of the most promising flat panel display technologies that are capable of meeting the demands of future display applications [2]. In particular, the OLED has advantages when applied to full color displays, backlight units of liquid crystal displays (LCDs) or as next generation lighting, [3] with white organic emitting diodes (WOLEDs) having high color rendering index (CRI) [4–6]. WOLED devices are specifically suitable for full color display using color filters with low eye strain white indoor lighting. The methods for the fabrication of WOLEDs can be classified according to the number of color dopant molecules in the emissive layer (EML). One of them is to mix two different

wave-length light emitting dopants in the EML [7–9] and the other is to obtain white emission by mixing three primary colors from red, green and blue dopants [10,11]. Two complementary color mixing method has the advantage of easy control of the CIE<sub>x,y</sub> color coordinates, but its application is limited for full color displays and as a lighting source due to the low CRI value. In contrast, three primary color mixing method provides a high CRI value and a broad spectrum. In regards to device structure, WOLEDs may be divided into two types; single-emissive layer (SEL) [12–14] and multi-emissive layer (MEL) [15–17] according to the EML's composition. Despite MEL showing a higher luminous efficiency than SEL, it has a possible shift of the CIE<sub>x,y</sub> coordinates with variations in applied voltage. This phenomenon occurs because of exciton recombination zone transfer in the EML as the applied voltage increases and it eventually leads to a shortened life-time of particular organic emissive layers and the whole EML. However, the SEL may have relatively more limited exciton recombination zones thus the potential shift of the CIE<sub>x,y</sub> coordinates is less than with the MEL, so that the device life-time is improved and perfect white color of CIE<sub>x,y</sub> coordinates (0.33, 0.33) are obtained. We can also adjust the energy transfer between the host and dopants by controlling the dopant concentration in the SEL WOLED. The Electrical and optical properties of the WOLED depends on the energy transfer between the host and dopants and it is affected by the energy band gap of the organic molecules in the EML. This energy transfer can be estimated through the

\* Corresponding author at: Department of Green Energy & Semiconductor Engineering, Hoseo University, Asan, South Korea. Tel.: +82 10 3116 0219.

E-mail address: [wykim@hoseo.edu](mailto:wykim@hoseo.edu) (W.Y. Kim).

observation of the peak overlap between the host molecule's emission spectra and the dopant's absorption spectra.

In this study, we fabricated SEL WOLEDs and achieved high luminous efficiency and stable white color coordinates. Energy transfer between the host and dopants was examined and estimated via UV–vis absorption and photoluminescence (PL) spectra. Experimentally measured color coordinates of the SEL WOLED were compared to those obtained from simulations using each emissive molecule's peak wavelength obtained by PL.

## 2. Experiments

Indium tin oxide (ITO) coated glass was cleaned in an ultrasonic bath by the regular cleaning sequence: in deionized water, isopropyl alcohol, acetone, deionize water, isopropyl alcohol, thereafter, the pre-cleaned ITO was treated with an O<sub>2</sub> plasma, under vacuum conditions of  $5.0 \times 10^{-2}$  Torr, of 50 W for 2 min. WOLED devices were fabricated by thermal evaporation under high vacuum conditions of  $5.0 \times 10^{-7}$  Torr. WOLEDs were composed of N,N'-diphenyl-N,N'-bis(1-naphthyl-phenyl)-(1,1'-biphenyl)-4,4'-diamine (NPB) as hole transport layer (HTL), 9,10-di(naphth-2-yl) anthracene (ADN) as host material, 4,4'-bis(9-ethyl-e-carbazovinylene)-1,1'-biphenyl (BCzVBi) as blue dopant, 10-(2-benzothiazolyl)-2,3,6,7-tetrahydro-1,1,7,7-tetramethyl-1H,5H,11H-(1)-benzopyrropano (6,7-8-i,j) quinolizin-11-one (C545T) as green dopant, 4-(di cyano methylene)-2-methyl-6julolidyl-9-enyl-4H-pyran (DCJTb) as red dopant, 4,7-diphenyl-1,10-phenanthroline (Bphen) as electron transport layer (ETL), and 8-hydroxyquinolinolato-lithium (LiQ) as the electron injection layer, respectively. Then the aluminum cathode electrode was deposited by thermal evaporation. The electro-optical characteristics of the WOLED devices were measured and observed using a Keithley 238 LMS PR-650 spectrophotometer, colorimeter and the IVL system. The color rendering index (CRI) was calculated by 'CIE 13.3:1995 Method of Measuring and Specifying Color Rendering Properties of Light Sources'. Fig. 1 shows the HOMO–LUMO energy band diagram of the SEL WOLED and Table 1 summarizes the device structures with different concentrations of dopants.

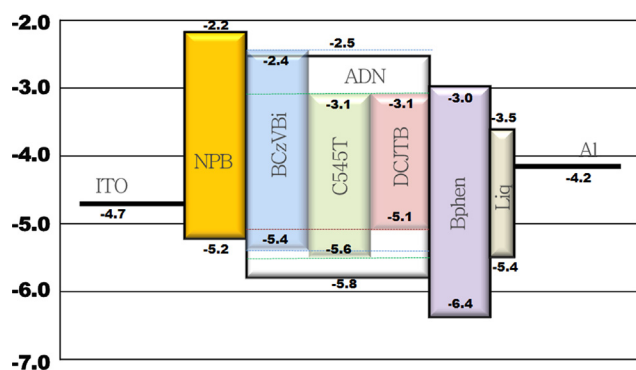


Fig. 1. HOMO–LUMO energy band diagram of WOLEDs.

## 3. Results and discussion

Fig. 2 shows the PL and absorption spectra of the host and three different RGB dopants, with their molecular structures inset. All the peaks of the organic molecule's absorption spectra were located at shorter wave-lengths than those of the photoluminescence (PL) spectra [18]. Usually, absorbed energy in fluorescent organic molecules excites electrons from the ground state to a higher excited state but releases energy to lower excited states throughout the internal conversion of the electron before relaxation and light emission [19]. The energy transfer between the host and dopants can be analyzed by the estimation of the peak overlap in the spectra of absorption and PL emission [20]. Electrons in the LUMO energy level of the host molecule are allowed to transfer into the dopant's LUMO energy level within a specific range of electron voltages which appear as peak overlap as described in Fig. 2. The calculated electron voltage value at the overlapped edge of the absorption and PL emission corresponds to the HOMO–LUMO energy band gap of each organic molecule. ADN as host has a larger energy band gap, of about 3.0 eV, than those of the dopants; BCzVBi, C545T and DCJTb. RGB emission spectra from BCzVBi, C545T and DCJTb were combined mathematically to obtain the white emission spectra as shown in Fig. 3(A). White emission was also calculated via the CIE<sub>x,y</sub> coordinates of RGB using a color matching function formula for R(λ), G(λ) and B(λ) shown in Fig. 3(B). [21] The CIE<sub>x,y</sub> coordinates of calculated white emission based upon RGB peak wave-length of the SEL WOLED's PL spectra is about  $(0.336 \pm 0.005, 0.324 \pm 0.005)$ , which is quite closed to the perfect white color coordinates of (0.33, 0.33).

The white color coordinates of (0.33, 0.33) is obtained by proper proportions of the RGB spectra, R(λ), G(λ) and B(λ) using a color matching function which corresponds to each wavelength intensity. To obtain perfect white emission, we need to assume energy transfer from host to dopants in the EML should increase with smaller energy gaps between their LUMO energy levels. According to this assumption, energy transfer occurs sequentially from ADN to BCzVBi, C545T, and then DCJTb. The degree of overlap between the absorption and PL emission peaks of the emissive materials is used to predict the energy transfer efficiency. Fig. 4 shows the overlap of the absorption and PL emission spectra between ADN–BCzVBi, BCzVBi–C545T, C545T–DCJTb.

Fig. 4(A) shows the lower degree of overlap between the emission peak of ADN and the absorption peak of BCzVBi, which suggests a less efficient energy transfer from the ADN host to the BCzVBi dopant molecules. Accordingly, the concentration of the BCzVBi dopant should be increased to improve the energy transfer in the EML. In contrast, as Fig. 4(B) indicates, the degree of overlap between the dopants BCzVBi and C545T as well as between C545T and DCJTb are relatively higher than between ADN and BCzVBi as shown in Fig. 4(B) and (C). Therefore, it is found that a high degree of overlap between the absorption and PL peaks generated from the dopants can occur in spite of a lower doping concentration in the EML [20]. Fig. 4(D) can be used to predict three types of energy transfer between energy donors and acceptors including ADN, BCzVBi, C545T and DCJTb, by showing overlap areas of 9.03%, 65.7%, and 53.13%. Assuming the sequential energy transfer happens from

Table 1  
Device structures of SEL WOLEDs.

	HTL(700 Å)	EML (300 Å)	ETL(300 Å)	EIL(20 Å)	Cathode
Device A	NPB	ADN:BCzVBi-7%:C545T-x% (x=0.05–1.0%)	Bphen	LiQ	Al(1200 Å)
Device B	NPB	ADN:BCzVBi-7%:C545T-0.05%:DCJTb-0.05%	Bphen	LiQ	Al(1200 Å)
Device C	NPB	ADN:BCzVBi-7%:C545T-0.05%:DCJTb-0.1%	Bphen	LiQ	Al(1200 Å)

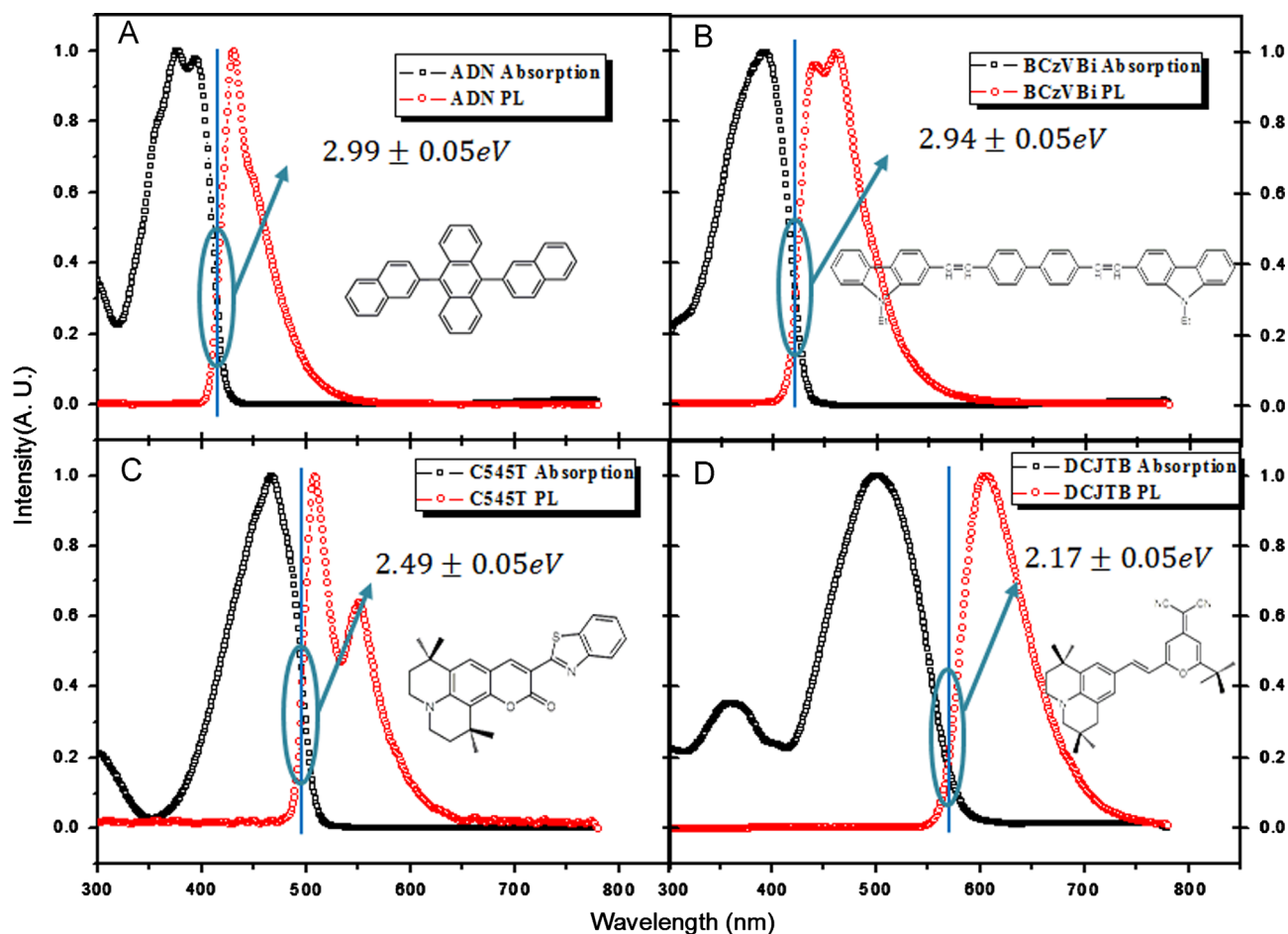


Fig. 2. UV-vis absorption and photoluminescence (PL) spectra of host and dopants.

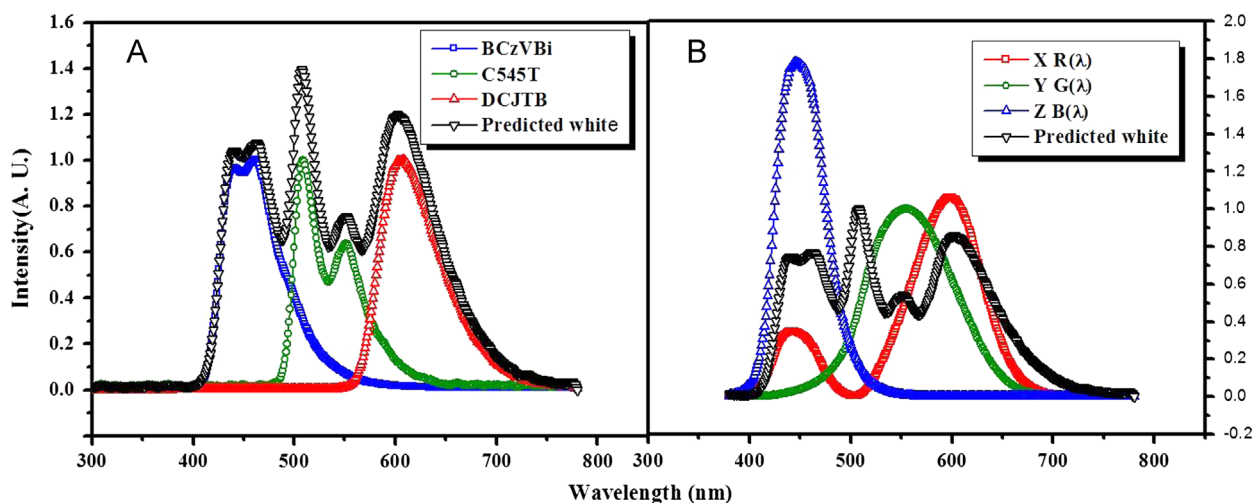


Fig. 3. (A) Predicted white emission spectrum (black line) combining the photoluminescence of RGB each dopant and (B) The relative ratio of predicted white emission spectrum (black line) based upon color matching function formula of  $R(\lambda)$ ,  $G(\lambda)$  and  $B(\lambda)$ .

ADN to DCJTb, we examined energy transfer between BCzVBi and C545T at a fixed 7% of BCzVBi dopant concentration which shows a high efficiency with no concentration quenching by changing the concentration of C545T. The changes in EL spectra of WOLED device A with changing the C545T doping concentration is shown in Fig. 5.

Device A without C545T doping shows a similar peak shape to the intrinsic EL spectrum of BCzVBi as shown in Fig. 2(B). However,

the green peak intensity of C545T appeared at 509 and 552 nm stays similar or grows gradually while BCzVBi's blue peaks at 452 and 476 nm become weaker with an increasing doping concentration of C545T. Considering the peak intensities of BCzVBi and C545T, device A with 0.05% of C545T is well balanced and optimized for energy transfer between the two dopants in the EML with a view to mix blue with green emission. This phenomenon is important to obtain better WOLEDs with a wide

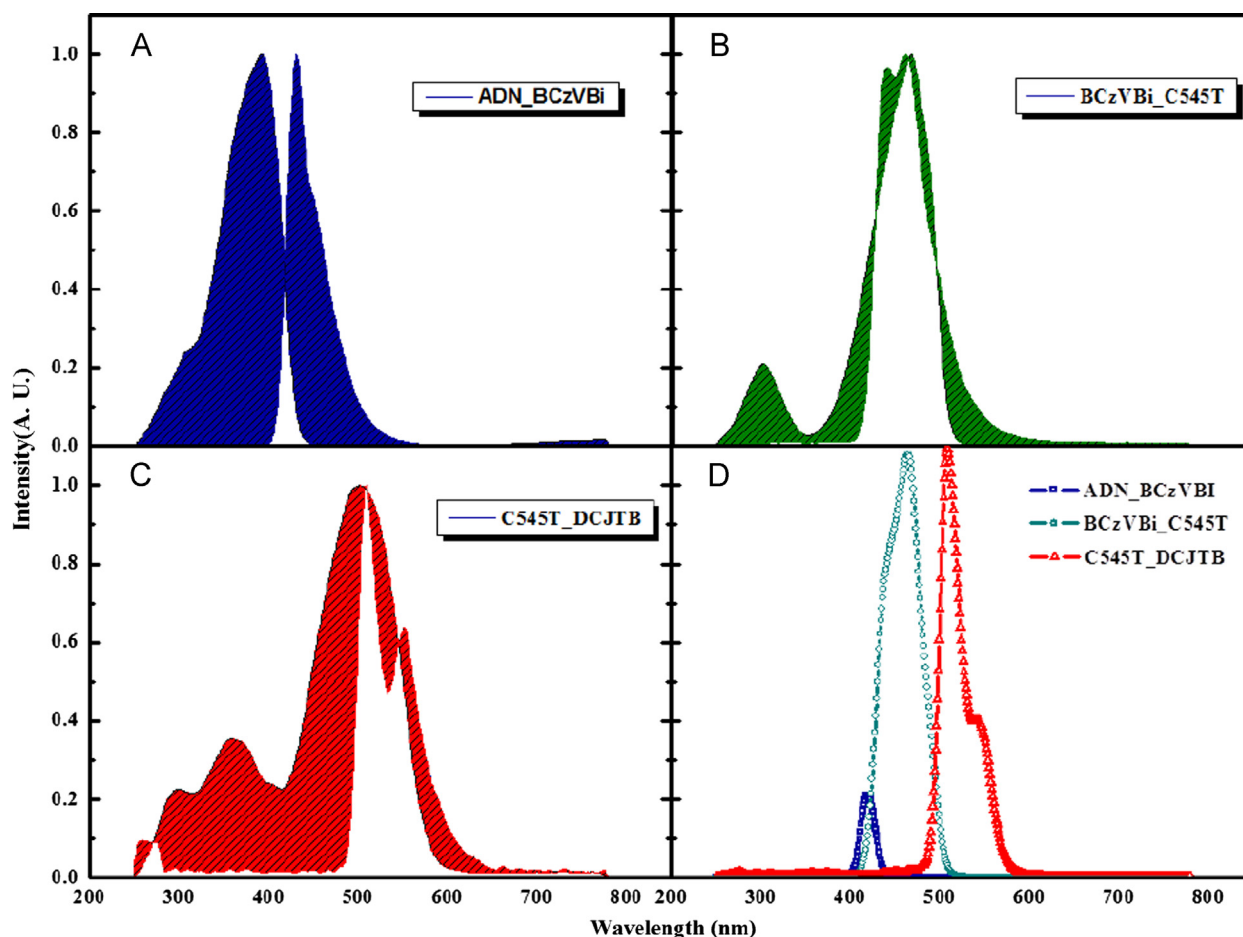


Fig. 4. The peak overlaps (white area) between PL and absorption spectra of emission materials. (A) AND's PL and BCzVBi's absorption, (B) BCzVBi's PL and C545T's absorption, (C) C545T's PL and DCJTb's absorption and (D) comparison of the peak overlaps in (A), (B) and (C).

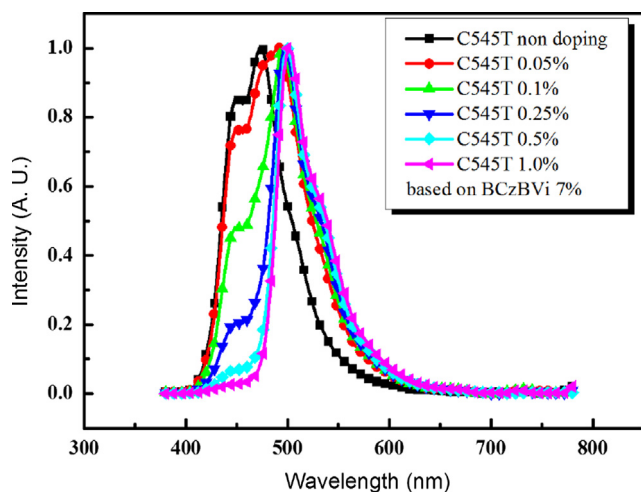


Fig. 5. EL spectra of SEL WOLED device A with 7% of BCzVBi as varying C545T's concentration.

wavelength EL spectrum. If C545T's concentration is higher than 0.05%, blue emission is not strong enough to render RGB color-balanced white OLEDs and their color coordinate are shifted to red region eventually. To fabricate perfect WOLEDs using RGB color mixing requires the addition of DCJTb as a red dopant along with blue BCzVBi and green C545T dopants. Devices B and C with 0.05% and 0.1% DCJTb concentrations were proposed to produce the best SEL WOLED structure as indicated in Table 1. The reason for the

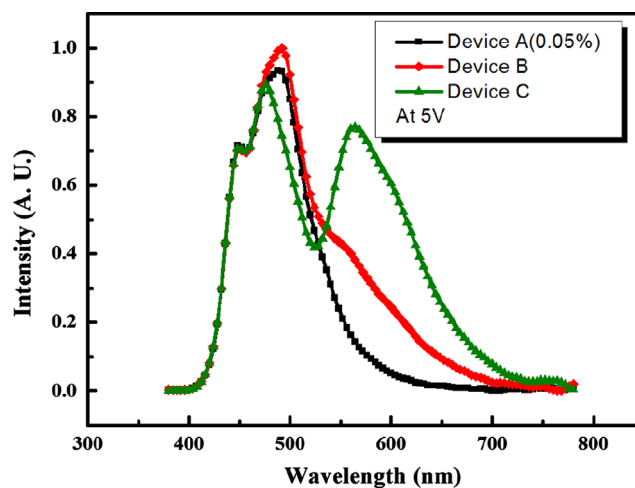


Fig. 6. EL spectra of devices A (0.05%), B and C.

low doping concentration of DCJTb given above is related to high energy overlap level between C545T and DCJTb

Fig. 6 shows the EL spectra of devices A, B and comparing peak patterns areas of the devices. Device C has a better peak balance of RGB colors to obtain white emission than the other devices. Device B has a red emission peak at 564 nm but it is not enough to achieve the required white color balance. The higher intensity of green emission at 509 nm is due to less energy transfer from C545T to DCJTb. C545T's green emission peak at 509 nm in Device

B is higher than in Device A because of the low concentration of DCJTb fully emits according to transferred energy from BCzVBi and then to C545T, whereas, device A emits by only BCzVBi and C545T. In other words, the relative intensity of the green emission of device B is higher than that of device A due to the relative amount

of energy transfer between the dopants. On the other hand, the EL spectrum of device C shows significant intensity of the red emission peak at 564 nm and reduction of C545T's green emission peak at 509 nm, which means most of the energy transfer from C545T to DCJTb is completed. The measured CIE<sub>x,y</sub> coordinates

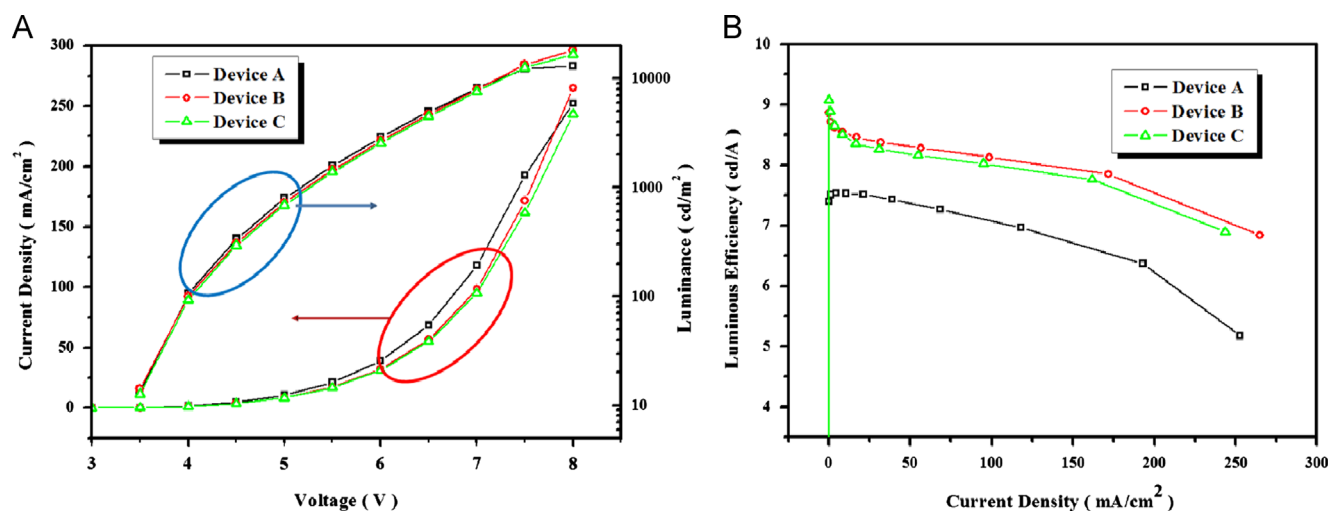


Fig. 7.  $I$ - $V$ - $L$  characteristics and luminous efficiency of WOLED devices A( $\chi=0.05\%$ ), B and C.

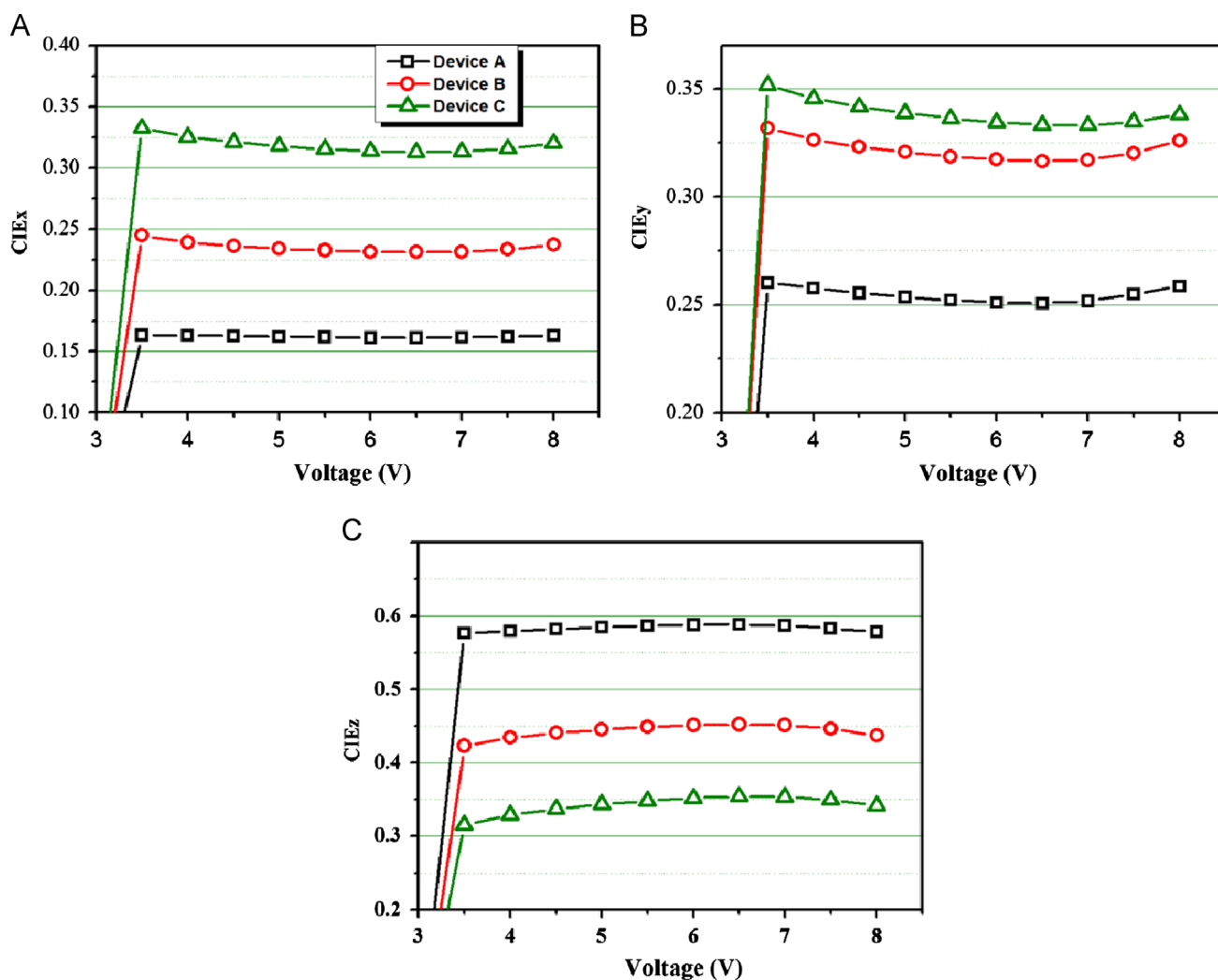


Fig. 8. CIE<sub>x,y,z</sub> coordinates of WOLED devices A, B and C with various voltages.



**Table 2**  
Color Rendering Index (CRI) of WOLED.

	5V	6V	7V	8 V
Device A*	13.33	12.80	12.91	13.74
Device B	50.00	51.16	50.95	51.96
Device C	81.38	81.01	81.39	82.77

\*  $x=0.05\%$

(0.320, 0.338) of WOLED device C and the predicted values ( $0.336 \pm 0.005$ ,  $0.324 \pm 0.005$ ) for white emission in Fig. 3 are very similar each other, considering minor experimental errors in doping concentration. The green emission does not significantly affect the  $CIE_{x,y}$  coordinates because of the lower value in the color matching function  $R(\lambda)$ ,  $G(\lambda)$  and  $B(\lambda)$  as mentioned earlier.

Fig. 7(A) shows the electrical properties of Device A, B and C. The current density–luminance–voltage curves of these devices have similar characteristics but the luminous efficiency of device A is significantly lower than devices B and C. Usually the current density of an OLED device is proportional to the concentration of charge carriers. The current densities of devices A, B and C are  $10.48 \text{ mA/cm}^2$ ,  $8.45 \text{ mA/cm}^2$ , and  $8.13 \text{ mA/cm}^2$  at 5 V, respectively, which implies their charge injection properties are similar to each other. Device A without DCJTb dopant shows a higher current density than device B and C because DCJTb has a lower carrier mobility caused by a number of trap levels in the molecule. Its low mobility of  $5.2 \times 10^{-6} \text{ cm}^2/\text{s V}$  affects  $I$ – $V$ – $L$  characteristics of the devices B and C [22]. Fig. 7(B) shows that the luminous efficiencies of devices B and C are higher than that of device A. The presence of the red dopant DCJTb increases the energy transfer efficiency between the dopants in the EML in spite of the lower current density. DCJTb generally affect as electrical impurities in EML because of low mobility and high energy gap compared with host material but luminous efficiency is improved due to increased probability of hole–electron recombination and remained energy after emission of C545T provides an opportunity to generate emission of DCJTb in EML. [23]  $CIE_{xyz}$  coordinates result from the color dependence proportion in the color matching function for  $R(\lambda)$ ,  $G(\lambda)$ ,  $B(\lambda)$  as indicated in Fig. 3(B). Fig. 8 shows the  $CIE_{xyz}$  coordinates of devices A, B and C with various applied voltages. At 6.5 V, the curve slopes of  $CIE_x$  and  $CIE_y$  are converted from negative (–) to positive (+) while that of  $CIE_z$  is reversed. This slope pattern means that the ratio of RGB emission depends upon the applied voltage. The  $CIE_x$  of device A has a constant value due to the lack of DCJTb red dopants. With regards to  $CIE_y$  of devices A, B and C, it is difficult to interpret the effect on emission by each of the dopants, C545T and DCJTb, because their emission peaks are located together in the region of 500–600 nm wavelength. We can more clearly explain the emission characteristics dependence on applied voltage by observing the  $CIE_z$  values. The  $CIE_z$  of device C increases until 6.5 V and then starts to decrease because the probability of electron–hole recombination increases under high concentration of BCzVBi but it decreases when the emission energy is saturated after 6.5 V. The  $CIE_z$  is reduced due to the transfer of energy to the other dopants, C545T and DCJTb. This type of  $CIE_{xyz}$  coordinate variation with applied voltage should happen more clearly in multi-emissive layer (MEL) WOLEDs than in SEL WOLEDs [24,25]. However, the variation of  $CIE_{xy}$  coordinates

in device B from 4 V to 8 V is only (0.005, 0.007) and it confirms high color stability.

Table 2 shows the variation of color rendering index (CRI) with applied voltage. We estimated the CRI of the WOLED devices based on Standard Illuminant Daylight 65(D65, CCT: 6500K). Device C has the highest CRI value of 82.77 at 8 V and the best white emission among the WOLED devices and less than 2% variation in the range of 5–8 V showing excellent color stability expected in SEL WOLED devices.

#### 4. Conclusion

We fabricated single emissive layer (SEL) WOLED devices using a host and three fluorescent dopants in the EML for three primary color mixture. High color stability of SEL WOLEDs was examined through color simulation, using the RGB peak wavelengths from the absorption and PL emission spectra. Optimized WOLED device C with host material ADN and dopants, BCzVBi, C545T and DCJTb produced a maximum luminance of  $16,800 \text{ cd/m}^2$  at 8 V and  $9.08 \text{ cd/A}$  at 3.5 V as well as white  $CIE_{xy}$  coordinates of (0.320, 0.338) and a color rendering index (CRI) of 82.77. The SEL WOLED is a promising device for use in LCD backlights and indoor planar lighting applications due to its color tunability and stability.

#### Acknowledgment

Following are results of a study on the “Leaders Industry–university Cooperation” Project, supported by the Ministry of Education, Science and Technology (MEST).

#### References

- [1] C.W. Tang, S.A. Vanslyke, *Appl. Phys. Lett.* 51 (1987) 913.
- [2] R.F. Service, *Science* 273 (1996) 878.
- [3] C.H. Chen, J. Shi, C.W. Tang, *Coord. Chem. Rev.* 171 (1998) 161.
- [4] P. Anzenbacher Jr., V.A. Montes, S.Y. Takizawa, *Appl. Phys. Lett.* 93 (2008) 163302.
- [5] Jwo-Huei Jou, Yi-Chieh Chou, Ching-Wu Wang, *J. Mater. Chem.* 21 (2011) 18523.
- [6] Jwo-Huei Jou, Shih-Ming Shen, J. Yung-Cheng, *Org. Electron.* 12 (2011) 865.
- [7] H. Kanno, R.J. Holmes, Y.R. Sun, S.K. Cohen, S.R. Forrest, *Adv. Mater. (Weinheim, Germany)* 18 (2006) 339.
- [8] B.W. D'Andrade, J. Brooks, V. Adamovich, M.E. Thompson, S.R. Forrest, *Adv. Mater. (Weinheim, Germany)* 14 (2002) 1032.
- [9] Y. Sun, N.C. Giebink, H. Kanno, B. Ma, M.E. Thompson, S.R. Forrest, *Nature (London)* 440 (2006) 908.
- [10] Seo Ji Hoon, Seo Ji Hyun, Yoon Sueng Soo, *Appl. Phys. Lett.* 90 (2007) 20.
- [11] Junhong Zhou, Na Ai, Jian Wang, *Org. Electron.* 12 (2011) 648.
- [12] R.S. Deshpande, V. Bulovic, S.R. Forrest, *Appl. Phys. Lett.* 75 (1999) 888.
- [13] Chihaya Adachi, Marc A. Baldo, S.R. Forrest, *J. Appl. Phys.* 90 (2001) 5048.
- [14] Brian W. D'Andrade, Russell J. Holmes, S.R. Forrest, *Adv. Mater.* 16 (2004) 7.
- [15] B.W. D'Andrade, M.E. Thompson, S.R. Forrest, *Adv. Mater. (Weinheim, Ger.)* 14 (2002) 147.
- [16] Ta-Ya Chu, Jenn-Fang Chen, *Appl. Phys. Lett.* 89 (2006) 113502.
- [17] Yung-cheng Tsai, Jwo-Huei Jou, *Appl. Phys. Lett.* 89 (2006) 243521.
- [18] A.B. Djurisic, T.W. Lau, W.K. Chan, *Appl. Phys. A* 78 (2004) 375.
- [19] C. Adachi, R.C. Kwong, Marc A. Baldo, *Appl. Phys. Lett.* 79 (2001) 2082.
- [20] Kim You-Hyun, Woo Young Kim, C.-B. Moon, *J. Appl. Phys.* 110 (2011) 034501.
- [21] Mark Shaw, Mark Fairchild, *Color Res. Appl.* 27 (2002) 316.
- [22] Haq Khizar-ul, Liu Shan-peng, W.Q. Zhu, *Semicond. Sci. Technol.* 23 (2008) 035024.
- [23] Hua-Ping Lin, Fan Zhou, Liang Zhang, *Synth. Met.* 161 (2011) 1133.
- [24] Young-Seo Park, Jae-Wook Kang, Jang-Joo Kim, *Adv. Mater.* 20 (2008) 1957.
- [25] Mei Meng, You-Hyun Kim, Woo Young Kim, *Nanosci. Nanotechnol. Lett.* 3 (2011) 131.